Improved Mesenchymal Stem Cells Attachment and *In Vitro* Cartilage Tissue Formation on Chitosan-Modified Poly(L-Lactide-*co*-Epsilon-Caprolactone) Scaffold

Zheng Yang, Ph.D.,[1,2] Yingnan Wu, M.Sc.,[2] Chao Li, B.Eng.,[3] Tianting Zhang, B.Sc.,[2] Yu Zou, B.Sc.,[2] James H.P. Hui, M.D.,[1,2] Zigang Ge, M.D., Ph.D.,[3,4] and Eng Hin Lee, M.D.[1,2]

Considering the load-bearing physiological requirement of articular cartilage, scaffold for cartilage tissue engineering should exhibit appropriate mechanical responses as natural cartilage undergoing temporary deformation on loading with little structural collapse, and recovering to the original geometry on unloading. A porous elastomeric poly L-lactide-co-ε-caprolactone (PLCL) was generated and crosslinked at the surface to chitosan to improve its wettability. Human bone marrow derived mesenchymal stem cells (MSC) attachment, morphological change, proliferation and *in vitro* cartilage tissue formation on the chitosan-modified PLCL scaffold were compared with the unmodified PLCL scaffold. Chitosan surface promoted more consistent and even distribution of the seeded MSC within the scaffold. MSC rapidly adopted a distinct spread-up morphology on attachment on the chitosan-modified PLCL scaffold with the formation of F-actin stress fiber which proceeded to cell aggregation; an event much delayed in the unmodified PLCL. Enhanced cartilage formation on the chitosan-modified PLCL was shown by real-time PCR analysis, histological and immunochemistry staining and biochemical assays of the cartilage extracellular matrix components. The Young's modulus of the derived cartilage tissues on the chitosan-modified PLCL scaffold was significantly increased and doubled that of the unmodified PLCL. Our results show that chitosan modification of the PLCL scaffold improved the cell compatibility of the PLCL scaffold without significant alteration of the physical elastomeric properties of PLCL and resulted in the formation of cartilage tissue of better quality.

Introduction

ARTICULAR CARTILAGE is an avascular connective tissue distinct from most tissues that has only limited self-regeneration ability. Chondral lesions that do not penetrate the underlying subchondral bone are unable to self-repair spontaneously due to the lack of migration of the resident chondrocytes and the progenitor cells from the blood or the bone marrow as a result of the absence of vasculature. With cell-based articular repair techniques such as autologous mesenchymal stem cell (MSC) implantation, repair and regeneration of knee joint cartilage with improved clinical outcome has been reported.[1–4] However, the neocartilage was a mixture of fibro and hyaline cartilage.[1–3] MSC derived cartilage has yet to achieve compatible biochemical content and mechanical strength to that of native cartilage.[5,6] Our work with the *in vivo* transplantation of MSC in a polycaprolactone scaffold in cartilage defects has shown significant neocartilage

formation with biomechanical compressive modulus in the range of native cartilage.[7] However, in cases where insufficient and inappropriate extracellular matrix (ECM) were formed, lower mechanical strength of the immature repair tissue subsequently contributed to degenerative changes.[7–11]

Articular cartilage is a weight-bearing tissue with viscoelasticity being one of the most important mechanical properties that endow cartilage with the unique capability to withstand continuous complex mechanical loading. Though the importance of mechanical compliance of scaffolds with native cartilage has long been recognized, to date few of the existing scaffolds could meet the requirements.[12] Most scaffolds used for cartilage repair are in the form of hydrogel or synthetic solid polymer. Although the biodegradable synthetic solid polymers have the advantage of improved mechanical strength, controllable degradation rate and easy manipulation, they often formed rigid and stiff scaffolds that are uncompressible. An ideal scaffold for cartilage

[1]Tissue Engineering Program, Life Sciences Institute, National University of Singapore, Singapore.
[2]Department of Orthopaedic Surgery, Yong Loo Lin School of Medicine, National University of Singapore, Singapore.
[3]Department of Biomedical Engineering, College of Engineering, Peking University, Beijing, P.R. China.
[4]Center for Biomaterials and Tissue Engineering, Academy for Advanced Interdisciplinary Studies, Peking University, P.R. China.

tissue engineering should exhibit appropriate mechanical responses as natural cartilage does, which undergoes temporary deformation on loading with little structural collapse, but recovers to the original geometry on unloading.[13]

An elastic biomaterial with appropriate mechanical strength will be able to meet this requirement. Several biodegradable elastomers, such as poly 1, 8-octanediol citrate and poly L-lactide-co-ε-caprolactone (PLCL), have been fabricated with elasticity.[13,14] However, the hydrophobic nature of the scaffolds has a drawback with the absence of cell recognition sites and they are not favorable for cellular interaction. In addition, the synthetic scaffolds adopted internal elasticity of the original polymers without mimicking cartilage structures and biochemical composition. In this study, we employed the mechano-active PLCL as the basal material of scaffolds. To create a biocompatible surface for cell attachment, we cross-linked de-acetylation (80%–95%) chitosan to the PLCL by using the aminolysis method to increase surface hydrophilicity.[15] Chitosan is a natural polysaccharide structurally similar to glycosaminoglycan (GAG) chains present in cartilage, and has been broadly applied to tissue engineering due to its intrinsic antibacterial activity, high biocompatibility, and mouldability.[16] Blending of chitosan with other biomaterials significantly altered the wettability and permeability of the resulting scaffold composite,[15,17] but inevitably changes the scaffold physical characteristic such as the porosity and the mechanical properties of the composite scaffold.[17,18] We took the approach of directly modifying the microenvironment of the PLCL scaffold itself by crosslinking the polymer surface with chitosan.[15]

The acquired scaffold has about 85% porosity with a good inter-connection between individual pores and a pore size of between 200 and 500 μm. Our previous study reported a significant improvement in scaffold swelling ratio, ability for chondrocyte attachment, and cartilage formation on the chitosan-modified PLCL.[15] In this study, the ability of the chitosan-modified PLCL scaffold to support MSC attachment, proliferation, and *in vitro* chondrogenesis was evaluated, in comparison to the unmodified PLCL scaffold. We provide cellular, biochemical, and mechanical evidence of PLCL/chitosan as a much improved scaffold for MSC-based cartilage tissue engineering.

Materials and Methods

Fabrication of PLCL and crosslinking of chitosan

A combination of porogen-leaching, freeze-extraction and lyophilization was adopted to fabricate three-dimensional scaffolds, as previously described.[11,12] Briefly, PLCL (LA:CL = 7:3; Mw 23,000 Da; Daigang Biomaterials, Inc.) was dissolved in 1, 4-dioxane (10% w/v), mixed with a proportional sodium chloride (NaCl), agitation, and cast at −20°C. The frozen mixtures were immersed in precooled 70% ethanol, the NaCl/PLCL mixtures were lyophilized, and NaCl was removed by dissolving in water. PLCL scaffolds were frozen at −20°C before being lyophilized.

An aminolysis method was used to immobilize chitosan in the PLCL scaffolds as previously described.[15] The scaffolds were sequentially treated with 50% ethanol, dried, then with 10% (w/v) 1,6-hexanediamine/isopropanol solution before being activated with 1% glutaraldehyde. The scaffolds were then incubated with 2 mg/mL chitosan (Guoyao Chemical Reagents Limited) solution (Degree of deacetylation 80.0–95.0%; viscosity 50–800 mPa.s; pH = 3.5) at 4°C for 24 h, then rinsed with 0.1 N acetic acid solution, followed by distilled water.

Measurement of scaffold hydrophilicity and porosity

The hydrophilicity of the PLCL and chitosan-modified PLCL was determined by contact angle measurement (θ). PLCL films were fabricated, and the water contact angles of the films were determined by a sessile drop method at 22°C by using a Water Contact Angle locator (SL-200B; Solon [Shanghai] information technology Co., Ltd.). A 5 μL droplet of water was placed on the surface of the film. All samples were measured for five times and results were shown as a mean value with standard deviation.

The scaffold porosity was estimated by having the exact sizes measured with a vernier caliper, and the masses of the scaffolds were taken. The scaffolds were then immersed in absolute alcohol for 2 h before being weighted again. Porosity was calculated as $(Ws - Wd)/ \rho/V$, where ρ represented the density of alcohol, V represented volume of the scaffolds, and Ws and Wd represent the weight of dry and wet scaffold respectively.

Degradation of scaffold

Scaffolds were placed at pH 7.4 in PBS (mass to volume ratio >10) in a shaking water bath at 37°C. The medium was replaced every third day. At 7, 14 and 21 days, scaffolds were taken from the solutions and washed thrice with distilled water to remove salts. The weight was measured after the scaffolds had been immersed in 100% ethanol for 2 h and dried for 1 day at room temperature. The percentage weight loss (%WL) of scaffolds was calculated as $\%WL = [(Wi - Wf)/Wi] \times 100\%$, where Wi is the initial dry weight of scaffold, and Wf is the weight of the dry scaffold after incubation in the PBS.

MSCs culture and chondrogenic differentiation

MSCs were generated from bone marrow aspirates of consented human donors. The bone marrow cells were washed with HBSS (Invitrogen), resuspended in Dulbecco's modified Eagle medium (DMEM) (Invitrogen) supplemented with 10% FBS (Invitrogen), and cultured at 37°C in 5% CO$_2$ atmosphere. After 72 h, nonadherent cells were removed. When reaching 70%–80% confluency, adherent cells were trypsinized and further expanded. A homogenous MSC population was obtained after 1–2 weeks of culture, and MSC was used between passage 3 and 5.

Chondrogenic differentiation media containing high glucose DMEM supplemented with 10^{-7} M dexamethasone (Sigma), 1% ITS + premix (BD Bioscience, Inc.), 50 mg/mL ascorbic acid, 1 mM sodium pyruvate (Sigma), and 4 mM proline (Sigma). Chondrogenic differentiation was induced in the presence of 10 ng/mL of TGFβ3 (R&D Systems). The cell/scaffold composite was cultured at 37°C in 5% CO$_2$ over a period of up to 5 weeks. Medium was changed every 3 days.

Cell seeding and assessment of cell attachment and spreading

The scaffold was surface activated with 70% ethanol, before being immersed in PBS until use. Before cell seeding, the

scaffold was blotted dry. MSC at 10×10^6 cell/mL were seeded onto the scaffolds ($4 \times 4 \times 2$ mm) immediately, allowed to adhere for 2 h before being cultured in MSC culture medium overnight. Cell attachment on scaffold was analyzed by scanning electron microscopy (SEM). Briefly, samples were fixed by paraformaldehyde and dehydrated through 50%, 75%, 95%, and 100% ethanol. Finally, the samples were washed by triethylsilane and air-dried overnight. Images of the cross-sectioned samples were taken with a JOEL 1000 SEM. To analyze cell cytoskeletal organization on the scaffold, the samples were fixed with 4% paraformaldehyde, permeabilized in 0.1% Triton X-100, and incubated with rhodamine phalloidin (Invitrogen) and 4′,6-diamidino-2-phenylindole (DAPI) before they were mounted and viewed under a confocal fluorescence microscope.

Cell proliferation

Cell proliferation in the scaffolds was evaluated by DNA quantification and Alamar Blue assays.

The DNA amount in cell/scaffolds was fluorometrically quantified by using Hoechst Dye 33258 solution.[19] Cell lysates were incubated with an equal volume of 0.1 mg/mL Hoechest 33258 (Molecular Probes, Invitrogen) solution for 10 min at room temperature, protected from light, in 96-well black plates. Fluorescence was determined by using a FLUOstar Optima fluorescent plate reader (BMG Labtech) at 350 nm excitation and 445 nm emission. DNA concentration in the samples was extrapolated from a standard curve generated using calf DNA.

The Alamar Blue assay is designed to quantitatively measure the proliferation of various human and animal cells.[20] Briefly, the medium in the wells was removed, and 10% Alamar Blue (Invitrogen) solution diluted in culture medium was added to the samples. The 10% diluted Alamar Blue culture medium served as the blank control. The samples were incubated in a CO_2 incubator for 2 h. The absorbance of the incubated Alamar Blue solution was measured by a microplate reader (TECAN, infinite M200) at a wavelength of 570 and 600 nm. The number of viable cells correlates with the level of dye reduction and is expressed as a percentage of Alamar Blue reduction, according to the manufacturer's protocol.

Sulfated GAG and type II collagen quantification

The cell/scaffold constructs were digested with 10 mg/mL of pepsin (Sigma) in 0.05 M acetic acid at 4°C for 5 day, followed by further overnight elastase (1 mg/mL, Sigma) digestion at pH 8.0. The digested solution was collected and kept at -20°C until assays. Triplicate samples from each treatment were analyzed based on two independent experiments.

The amount of sulfated glycosaminoglycan (sGAG) was qualified by using Blyscan sGAG assay kit (Biocolor Ltd.) following the manufacturer's protocol. The digested solution was mixed with Blyscan dye and placed on a mechanical shaker for 30 min. The precipitate was collected by high speed centrifugation, unbound dye completely removed, and dissolved in dissociation reagent. The absorbance of re-dissolved dye was measured in 96-well plates by using FLUOstar Optima plate reader at an absorbance wavelength of 656 nm. The standard curve of sGAG was generated from sGAG standard solution supplied by manufacture.

Type II collagen was measured by using a captured enzyme-linked immunosorbent assay (ELISA; Chondrex), according to the manufacturer's protocol. Measurement was taken on a TECAN Infinite M200 at an optical density of 490 nm, and a concentration of collagen was extrapolated from a type II collagen standard curve (supplied with the kit).

Histological and immunohistological assessment

The samples were washed with phosphate buffered saline (PBS) and embedded with Tissue Freezing Medium® (Leica). Cryosections of 10-μm were prepared by using Leica Cryostat Microtome (Leica CM3050 S). The cut sections were then fixed in an ice-cold mixture of acetone and methanol (1:1, v:v) before histological and immunological staining.

For alcian blue staining, the tissue sections were incubated with 0.5% alcian blue (Sigma) in 0.1M HCl and counterstained with nuclear fast red (Sigma). For immunohistochemistry staining, endogenous peroxidase in the tissue sections was blocked with hydrogen peroxide before pepsin treatment. Monoclonal antibodies of collagen type II (Col2, Clone 6B3; Chemicon, Inc.) of dilution factor 1:500 was applied followed by incubation with biotinylated goat anti-mouse (Lab Vision Corporation). Streptavidin peroxidase was added, 3,3′-diaminobenzidine was used as a chromogenic agent, and counterstaining was done with Gill's hematoxylin. The slides were dehydrated before being coverslipped.

Real-time PCR analysis

Samples were digested in 0.25% collagenase solution at 37°C for 2 h. Cells were collected by centrifugation, and total RNA was extracted by using the RNeasy Mini Kit (Qiagen) following the manufacturer's protocol. RNA concentration was determined by using the NanoDrop (NanoDrop Technologies), and reverse transcription reactions were performed with 50 ng total RNA using iScript™ cDNA synthesis kit (Biorad Laboratories). Real-time PCRs were conducted by using the SYBR green system. Primer set sequences were as follows: GAPDH(F): 5′-ATGGGGAAGGTGAAGGTCG-3′; GAPDH(R): 5′-TAAAAG CAG CCCTGGTGACC-3′; collagen II(F): 5′-GGCAATAGCA GGTTCACGTACA-3′; collagen II(R): 5′-CGATAACAGTCTTG CCCCACTT-3′; Aggrecan(F): 5′-ACTTC CGCTGGTCAGAT GGA-3′; Aggrecan(R): 5′-TCTCGTGCCAGATCATCACC-3′. Real-time PCRs using the ABI 7500 Real-Time PCR System (Applied Biosystems) were performed at 95°C for 10 min, followed by 40 cycles of amplifications, consisting of a denaturation step at 95°C for 15 s, and an extension step at 60°C for 1 min. The level of expression of the target gene, normalized to glyceraldehyde-3-phosphate dehydrogenase (GAPDH), was then calculated by using the $2^{-\Delta\Delta Ct}$ formula with reference to the undifferentiated MSC.

Mechanical analysis

Compression tests of the scaffold constructs were undertaken, and the porcine full-thickness articular cartilages were used as control. The scaffolds and porcine cartilage were collected and equilibrated in PBS before a compression test. A compression test was carried out with Bose ELF 3200 (Bose Corporation). Compressive loads were applied by using a stainless steel indenter (Honeywell Sensotee; mode 31, max. loading 10N, diameter = 1.97 mm). All the samples were
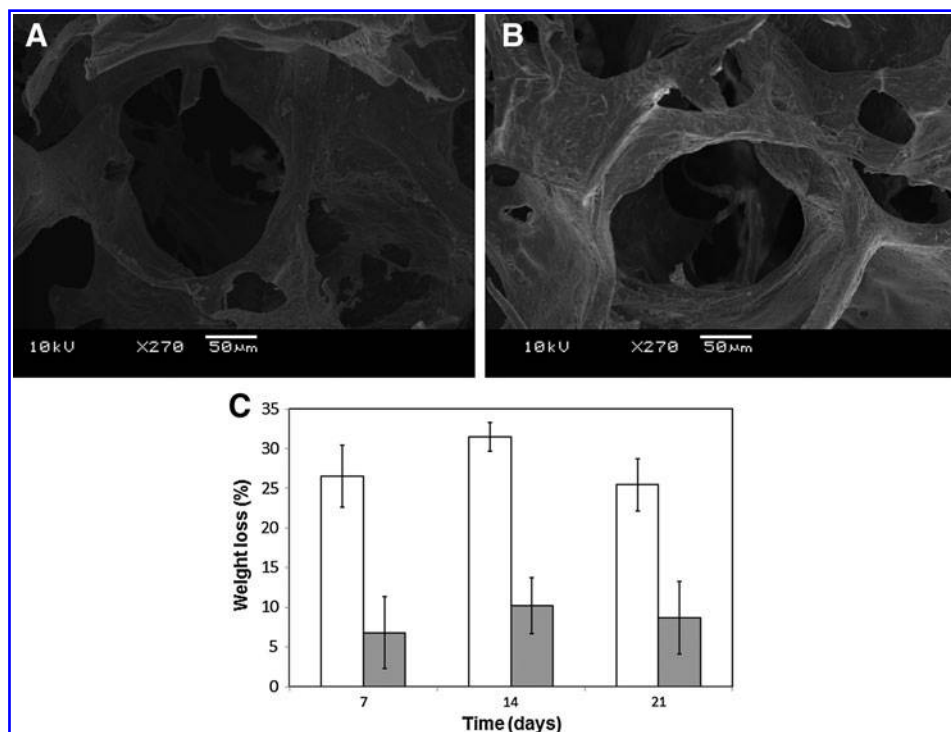
FIG. 1. Scanning electron microscopy (SEM) microphotographs of poly L-lactide-co-ε-caprolactone (PLCL) **(A)** and PLCL/chitosan **(B)** scaffold. Weight loss percentage of PLCL (white bar) and PLCL/chitosan (gray bar) at days 7, 14, and 21 **(C)**. Scaffolds were embedded in PBS at 37°C. Values are reported as mean±SD ($n = 3$).

tested at five different points. The samples were loaded at 0.01 mm/s until the 15% strain was reached. The measured thickness was converted to the strain of the sample ($\varepsilon = 1 - L/L0$, where L0 and L represent the thickness before and after compression, respectively). Young's modulus ($E = \sigma/\varepsilon$, where σ and ε denote the stress and strain of the sample, respectively) was determined by Microsoft Excel on the stress–strain plot.

Statistical analysis

Statistical significance was calculated by using student's *t*-test. Data were presented as the mean±SD, with the level of significance set at $p < 0.05$. All quantitative data reported here were averaged from two to three independent experiments.

Results

Characterization of scaffolds

SEM microphotographs show increasing surface roughness of the chitosan-modified PLCL (PLCL/chitosan) (Fig. 1A, B) without significant changes to the porosity of the scaffolds[15] (Table 1). Wettability estimation of the two scaffolds shows a significant decrease in contact angle of water droplets on the PLCL/chitosan surface (Table 1), thus indi-

Table 1. Porosity, Wettability, and Mechanical Properties of The Scaffold

	PLCL	PLCL/chitosan
Porosity (%)	85.5±7.9	84.5±8.2
Contact angle (θ)	89.67±3.41	62.50±4.79[a]
Young modulus (kPa)	84.1±12.5	128±16.9[a]
Recovery ratio	0.898±0.049	0.958±0.040

[a]$p < 0.05$ when compared with value of PLCL.
PLCL, poly L-lactide-co-ε-caprolactone.

cating an increase in surface hydrophilicity after PLCL was modified with chitosan. The elastic mechanical properties of the PLCL/chitosan expressed in Young's modulus and the recovery ratio was similar to the unmodified PLCL (Table 1).

Degradation rate of the scaffolds was determined by the percentage of weight loss of scaffolds after incubating at 37°C in PBS over a period of 3 weeks. Chitosan modification of PLCL has rendered the scaffold less susceptible to degradation (Fig. 1C), probably a result of increase cross-linking by the glutaraldehyde treatment during modification procedure.

Cell proliferation, attachment, and morphology in the scaffold

We then examined the interaction of the MSC within the scaffolds. To evaluate the attachment of MSC onto the scaffold, cells were seeded to the scaffold, and SEM microphotographs were taken at 16 h postseeding. Figure 2B shows that MSCs on PLCL/chitosan scaffold were elongated and well spread. Comparatively, MSCs on PLCL scaffold remained less spread and adopted a much rounder morphology (Fig. 2A, indicated by arrows). Noticeably, areas of the PLCL surface were not occupied by MSCs (Fig. 2A, indicated by arrowheads). The cytoskeleton organization of the MSCs was shown by phalloidin staining of the F-actin in Figure 3. MSCs on the PLCL/chitosan scaffold formed stress fiber in the cytoplasm and adopted a spread morphology as early as 16 h postseeding (Fig. 3D) and extensive cell-cell interaction at 72 h (Fig. 3E). Comparatively, MSC on the PLCL scaffold were mostly unspread and did not stain strongly with phalloidin, thus indicating a lack of actin polymerization at 16 h (Fig. 3A, indicated by arrowheads). The few cells attached to the PLCL surface were elongated and had F-actin visible on the membrane of cells (Fig. 3A, indicated by arrows). MSCs on the PLCL scaffold only adopted a spread-up morphology and formed either regional punctuated F-actin fiber (Fig. 3B) or stress fiber (Fig. 3C) by 72 h

FIG. 2. SEM microphotographs of mesenchymal stem cells (MSCs) attached on PLCL **(A)** and PLCL/chitosan **(B)** scaffold taken 16 h postseeding. Arrowheads refer to regions of scaffold surface devoid of cells, and arrows refer to attached cells. Alamar blue assay **(C)** for proliferation of MSCs cultured on PLCL (white bar), PLCL/chitosan (gray bar) scaffolds at 1, 3, 5, and 7 days.
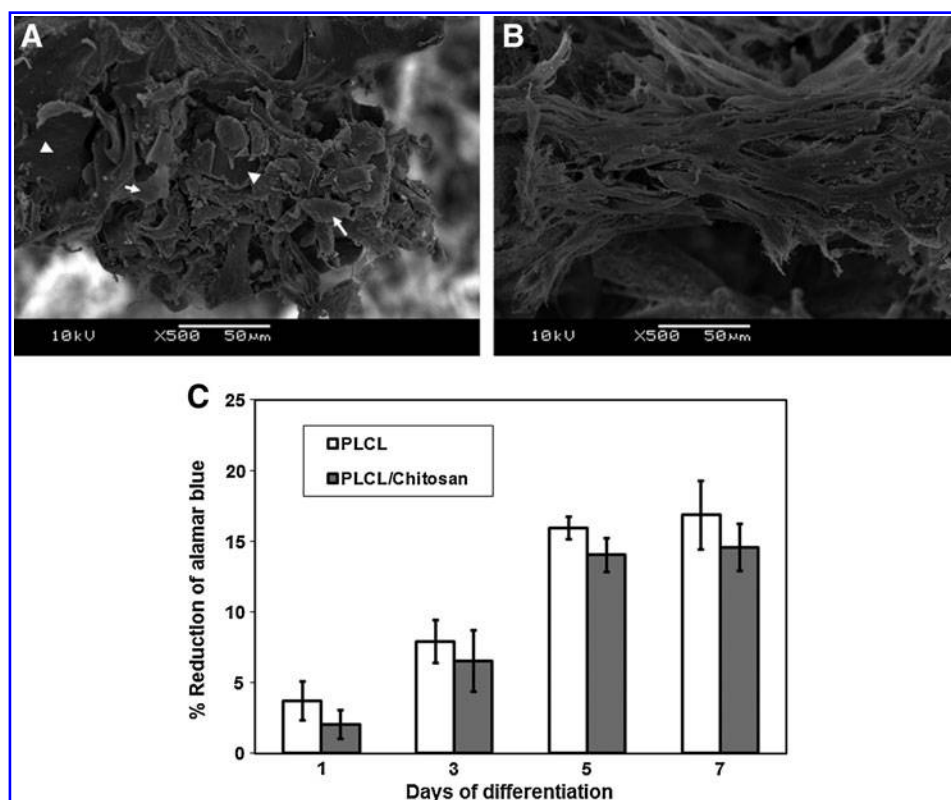
after seeding. Notably, at 72 h, there was congregation of aggregated cells protruding from the layer of stretched cells in the PLCL/chitosan scaffold (Fig. 3F, region indicated by dotted line). These aggregated cells had lost their F-actin stress fiber, unlike the underlying cells, and had their actin cytoskeleton reorganized into a cortical pattern.

MSCs remained metabolically active and continued to proliferate in both scaffolds, as shown by the Alamar Blue assay (Fig. 2C). There was no significant difference in dye reduction between the PLCL and PLCL/chitosan samples at all time points up to 7 days, thus indicating similar proliferate activity on both scaffolds.

FIG. 3. Cell cytoskeletal organization of MSC in PLCL **(A–C)** and PLCL/chitosan **(D–F)** scaffolds at 16 **(A, D)** and 72 h **(B, E, C, F)**. Actin was stained red and the cell nucleus was stained blue. Images were taken at ×600 magnification. Arrowheads refer to unspread cells, and arrows refer to elongated cells. Dotted lines indicates region of aggregated cells.
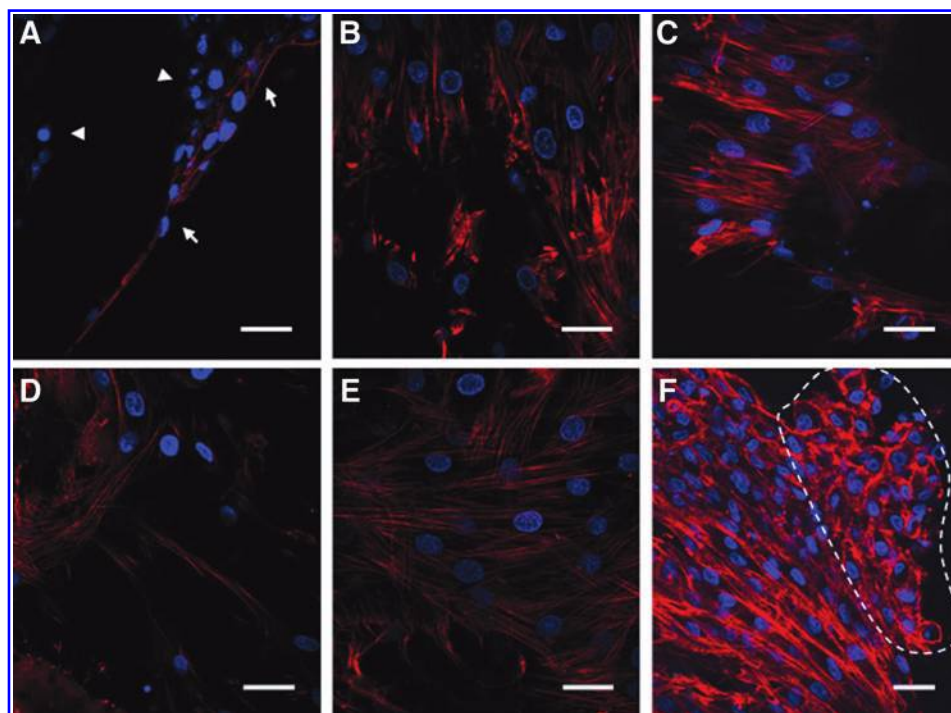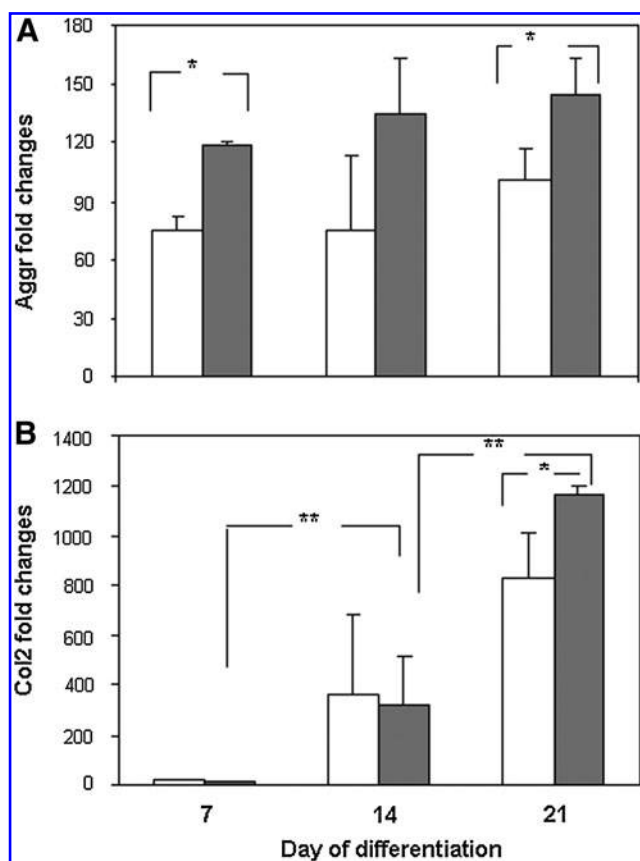
FIG. 4. Real-time PCR quantification of chondrogenic marker aggrecan **(A)** and type II collagen (Col2, **B**) in MSC-PLCL (white bar) and PLCL/chitosan (gray bar) constructs. Expression was normalized to GAPDH and presented as fold changes relative to level in undifferentiated MSC. Data shown are means ± SD ($n = 5$). *$p < 0.05$ significant increase in PLCL/chitosan construct compared with PLCL construct. **$p < 0.05$ significant increase between time points.

Evaluation of chondrogenic differentiation of MSC and cartilage ECM formation in the scaffold

MSCs seeded onto the scaffolds were allowed to undergo chondrogenic differentiation for up to 21 days. Real-time PCR results in Figure 4 show an increase in mRNA expression of chondrogenic markers aggrecan and Col2 in both PLCL and PLCL-chitosan. When comparing levels of expression between the two types of scaffolds at all time points, expression levels of aggrecan ($p = 0.011$ at day 7 and $p = 0.036$ at day 21) and Col2 ($p = 0.037$ at day 21) in PLCL/chitosan samples were significantly higher than PLCL samples. In addition, significant time-dependent increase expression of Col2 (from day 7 to day 14 and from day 14 to day 21, both at $p = 0.020$) was detected in PLCL/chitosan samples.

MSC seeded onto the scaffolds that had been allowed to undergo chondrogenic differentiation up to 28 days was histologically and immunohistochemically analyzed to evaluate for ECM formation. Figure 5C and D show mature cartilaginous ECM formation in the PLCL/chitosan construct, indicated by an abundant accumulation and widespread deposition of sGAGs and Col2 in the construct. Comparatively, cartilage tissue formation in the PLCL/chitosan samples penetrate almost the full depth of the 2 mm thick scaffold, contrasting to that of the PLCL samples (Fig. 5A, B), in which tissue formation was found to localize either near the surface of the scaffold or only at parts of the scaffold. Vast regions in the PLCL scaffold were devoid of cells as indicated by the lack of cellular counter staining in Figure 5A and B, indicative of poor cell distribution in this scaffold.

Quantification of sGAG by DMB assays shows significantly higher amount of total sGAG formation in the PLCL/chitosan construct than the PLCL construct (Fig. 6A, $p = 0.032$ and $p = 0.007$). Notably, the time-dependent increase in sGAG was obvious and significant with the PLCL/chitosan construct ($p = 0.006$) but not significant in the PLCL construct ($p = 0.35$). Col2 in the constructs was quantified by ELISA, thus showing a significant increase in total Col2 accumulation in the PLCL/chitosan construct than the PLCL samples at all time points (Fig. 6B, $p = 0.019$ and 0.018). Notably, earlier and higher quantity of collagen (>10-folds at day 14) was detected in the PLCL/chitosan construct than the PLCL construct. Although a significant time-dependent increase in Col2 was detected in both scaffold constructs, the amount of Col2 protein detected in the PLCL/chitosan construct was more consistent as attested by the small standard deviation.

A significant increase in DNA level was detected in the PLCL/chitosan construct at both differentiation time points
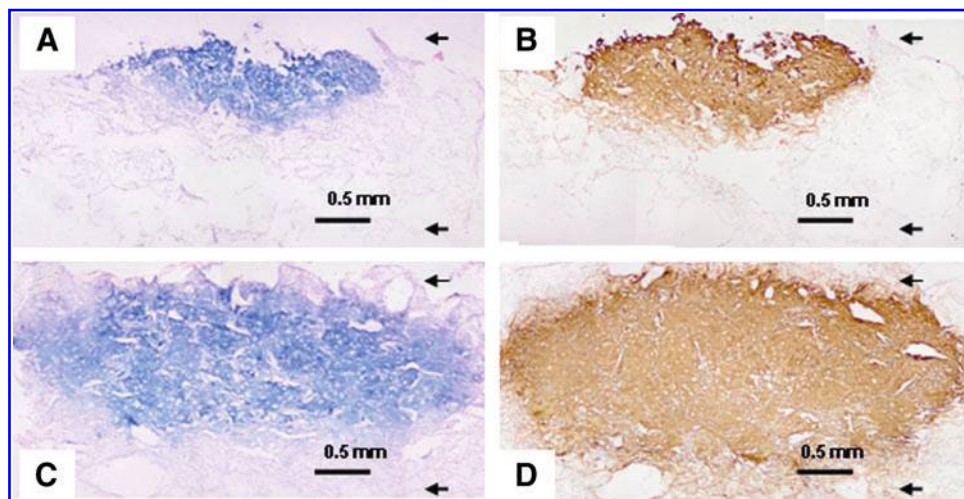

FIG. 5. Histological studies of MSC-PLCL **(A, B)** and PLCL/chitosan **(C, D)** constructs after 4 weeks differentiation. The sections were stained with alcian blue **(A, C)** or type II collagen **(B, D)**. Arrows in the images denote the top and bottom of the scaffold.
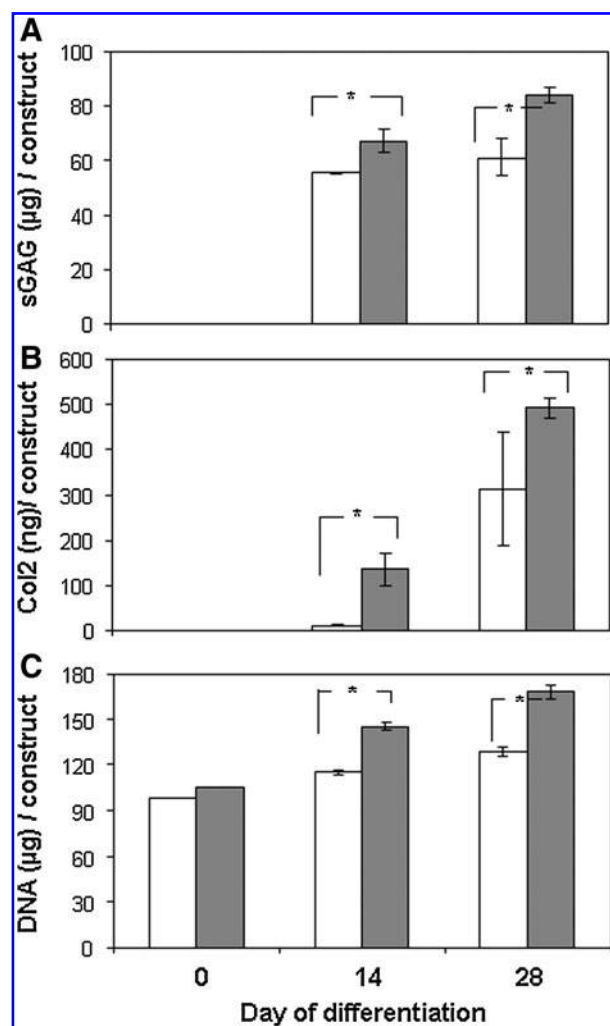
FIG. 6. Quantification of chondrogenic differentiation of MSC in PLCL (white bar) and PLCL/chitosan (gray bar) constructs after 2 and 4 weeks differentiation. **(A)** Total sulfated glycosaminoglycan (sGAG), **(B)** total Type II collagen, and **(C)** total DNA in the scaffold construct. Data shown are means±SD ($n=5$). *$p<0.05$ significant increase in PLCL/chitosan construct compared with PLCL construct.

of 14 and 28 days (Fig. 6C), thus indicating an increase in cell proliferation in the PLCL/chitosan construct with extended differentiation period.

Evaluation of mechanical strength of the cell/scaffold construct

Scaffolds seeded with MSC that had been allowed for 5 weeks of chondrogenic differentiation were subjected to a compression test to assess the mechanical properties of the resulting tissues. As reported by our previous study, the compression modulus of the empty PLCL/chitosan scaffold was significantly higher than the unmodified PLCL ($p=0.22$). Figure 7 shows that with tissue formation, the Young's modulus of the cell/PLCL construct was 386.3 ± 97.3 kPa ($n=5$) compared with the empty PLCL scaffold (84.1 ± 12.5 kPa, $n=3$), registering an increase of >4 fold. The Young's modulus of the cell/PLCL/chitosan construct was 735.3 ± 210 kPa ($n=5$) compared with the empty
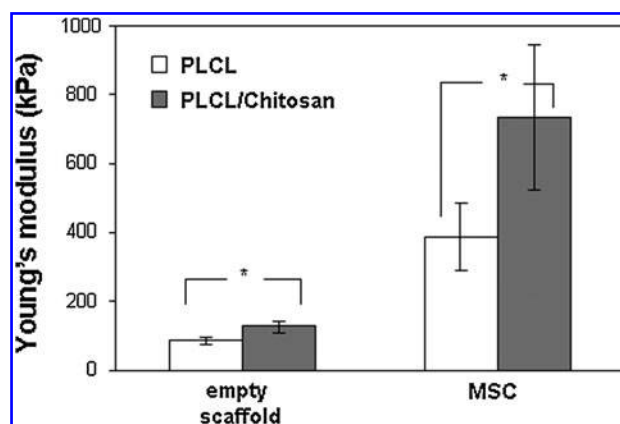

FIG. 7. Young's modulus of PLCL (white bar), PLCL/chitosan (gray bar) scaffolds, and MSC-PLCL (white bar), PLCL/chitosan (gray bar) constructs after 5 weeks of differentiation. Data shown are means±SD ($n=5$). *$p<0.05$ significant increase in PLCL/chitosan construct compared with PLCL construct.

PLCL/chitosan scaffold (128 ± 16.9 kPa, $n=3$), registering an increase of >5-fold. The compressive modulus of the cell/PLCL/chitosan tissue construct has achieved a compressive modulus nearly double that of tissue construct formed on the unmodified PLCL ($p=0.010$). However, the compressive strength of the PLCL/chitosan construct was at least 10-fold less than that of a native full-thickness cartilage tissue (~10 MPa), measured using the same parameter.

Discussion

Using the straight forward chemically crosslinking of chitosan to the surface of the PLCL scaffold, we increased the surface roughness and the surface hydrophilicity of the PLCL scaffold, without altering the scaffold porosity, and the elastic nature of the PLCL was not compromised. The improved wettability and permeability of the PLCL/chitosan promoted even distribution of the seeded MSCs throughout the scaffold. Recent publications have demonstrated that small changes in matrix hydrophobicity through modification of surface chemistry can dramatically alter cell-matrix interaction, thus making a profound impact on cellular behaviors such as adhesion, morphology, motility, cytoskeletal organization, and differentiation.[21,22] MSC seeded on the more hydrophilic chitosan-modified surface adopted an earlier spread-up morphology with extensive stress-fiber, probably exerting a positive effect in cell–cell interaction. Rapid reorganization of the actin cytoskeleton is one of the primary cellular responses to many extracellular signals and during cell-cell interaction.[23] The early and extensive cell-cell interaction in the PLCL/chitosan was followed by subsequent reorganization of actin cytoskeletal to the cortical with a concomitant rounding of cells forming cell aggregation, an event reported to associate with the activation of stem cells chondrogenic differentiation.[24–26] Taken together, our data indicate that provision of the scaffold surface with chitosan coating greatly enhanced MSC distribution in the scaffold. The strikingly different morphology acquired by the MSCs on attachment to the two scaffolds might have a direct effect on subsequent differentiation.

Chondrogenic differentiation of MSC took place in both PLCL and the chitosan modified scaffolds, as shown by the increase of expression in the chondrogenic markers and the formation of cartilaginous ECM proteins. Despite not detecting difference in cellular proliferation at earlier differentiation time points (Fig. 2C), cells in PLCL/chitosan construct were able to proliferate better during the extended period of differentiation (Fig. 6C). This was probably due to the even cellular distribution within the PLCL/chitosan scaffold, thus ensuring accessibility to sufficient nutrient supply contributing to the increase in cell proliferation during prolonged culture, and widespread as well as quantitatively more robust ECM deposition within the PLCL/chitosan construct. In contrast, the confined high congregation of cells within a small region in the PLCL scaffold might have caused a deficit in nutrient supply locally, thus impeding long-term cellular proliferation. On the other hand, the lack of critical MSC mass in the rest of the PLCL scaffold prevented these loosely distributed cells from undergoing proper cellular condensation and chondrogenic differentiation,[6,27,28] thus resulting in an overall lower total ECM formation within the PLCL construct.

The early induction of differentiation, coupled with the even distribution of cells within the PLCL/chitosan scaffold, resulted in significant increment of overall ECM deposition and tissue compressive strength. Our PCR analysis that determined the levels of chondrogenic markers expressed by seeded cells within the scaffold detected an increase expression of aggrecan and Col2 in the PLCL/chitosan samples, indicating that, indeed, MSCs within the chitosan-modified scaffold had undergone more robust chondrogenic differentiation. However, since cells in the porous scaffolds might have their secreted ECM diffused into the surrounding medium, which could be further affected by the degradation profile of the scaffold, we cannot rule out that the increase in ECM deposition within the PLCL/chitosan scaffold might be in part due to the lower degradation rate of the PLCL/chitosan scaffold compared with the unmodified PLCL. In addition, the chitosan modification had rendered the PLCL surface with an increase in hydrophilicity and high positive charge, both properties known to have a positive impact on protein and proteoglycan adsorption,[22,16] and might also contribute to the increase in retention of ECM. Compared with attempts by others to improve cell distribution in the scaffold either by embedment of cell in hydrogel before seeding onto the PLCL scaffold,[29–31] or the employment of a compression force–induced suction that required a custom-designed loading apparatus,[32] our chitosan-modified PLCL scaffold offers an operative improvement that allows direct cell seeding to the PLCL scaffold while retaining the mechano-active nature of the PLCL elastomeric properties. The chitosan modification has improved the surface properties of the PLCL in terms of wettability and ionic charge, together with its positive effect in inducing MSC chondrogenic differentiation, these altered surface properties might exert an overall enhancing effect in cell-deposited ECM within the construct.

Despite the enhancement of ECM production and compressive modulus on PLCL/chitosan scaffold, our *in vitro*-generated cartilage construct was still inferior to normal cartilage, probably being attributed to the relatively insufficient levels of both the proteoglycan and collagen in the neocartilage in comparison to native cartilage, as mechanical properties of cartilage depend on the content and structure of ECM.[33,34] Further improvement of the current scaffold should be considered including endorsing the microenvironment of the scaffold with biochemical features that better mimic the cartilage ECM to facilitate stem cell chondrogenesis and ECM deposition. The chitosan coating creates an electropositively charge environment that is unlike that of the cartilage electronegative microenvironment from the abundant sGAG chains of proteoglycans. The current scaffold also has absence of collagen structure which is known to provide biochemical signals that promote chondrogenesis.[35,36] Our earlier work comparing MSC chondrogenic differentiation on various cartilaginous ECM components crosslinked to the highly reactive amine groups in chitosan-modified alginate microbeads has identified both Col2 and chondroitin sulfate to improve cartilage ECM formation.[37] The current chitosan-modified PLCL provides a platform in which various cartilaginous components can be ionically complexed to the PLCL backbone to further explore the contribution of the biomimetic microenvironment. The chitosan-modified PLCL scaffolds, although having similar viscoelasticity with cartilage and relatively good recovery ratio from compression deformation, are still mechanically weaker when compared with cartilage.[15] Further enhancement of the compressive Young's modulus of the PLCL material by blending with other materials will have to be explored. More critically, since cartilage is a weight-bearing tissue in which cells within the tissue are under constant compressive stress, incorporating a dynamic compressive system that simulates physiological compressive situations during stem cell differentiation will better reflect the contribution of a mechano-active scaffold such as PLCL to stem cell chondrogenic differentiation. Transfer of proper mechanical signals to chondrocytes and MSC within the scaffolds is beneficial, as cyclic mechanical stimuli have been shown to enhance ECM formation and mechanical strength of the tissue.[10,33,38] With the mechano-active elastomer PLCL, dynamic compressive stimulation with chondrocytes[39] and MSCs[40] laden in the scaffold has resulted in enhanced ECM protein expression and compressive modulus of the tissue generated, compared with the cell/scaffold at static condition. Future studies should adopt a dynamic compressive stimulation system to study the chondrogenic differentiation of MSCs laden in our scaffold composites.

In conclusion, this study demonstrated that provision of the elastic PLCL scaffold with chitosan coating improves the cell compatibility of the scaffold. The resulting PLCL/chitosan scaffold has improved wettability and permeability for cell attachment and distribution. The morphology MSC adopted on attachment to the PLCL/chitosan scaffold might have provided an early induction of differentiation. Together with the consistent and even cellular distribution of MSC within the PLCL/chitosan scaffold, this resulted in an improvement in cellular proliferation and more robust cartilage tissue formation in terms of wider spread of ECM deposition in the construct, larger quantities of proteoglycan and Col2 production, and an overall increase in the compressive strength of the tissue construct. Our chitosan-modified PLCL scaffold demonstrates an operative improvement that allows direct cell seeding to the PLCL scaffold and formation of cartilage with better quality.

Disclosure Statement

No competing financial interests exist.

References

1. Wakitani, S., Goto, T., Pineda, S.J., Young, R.G., Mansour, J.M., Caplan, A.I., and Goldberg, V.M. Mesenchymal cell-based repair of large, full-thickness defects of articular cartilage. J Bone Joint Surg Am **76,** 579, 1994.

2. Wakitani, S., Imoto, K., Yamamoto, T., Saito, M., Murata, N., and Yoneda, M. Human autologous culture expanded bone marrow mesenchymal cell transplantation for repair of cartilage defects in osteoarthritic knees. Osteoarthritis Cartilage **10,** 199, 2002.

3. Kuroda, R., Ishida, K., Matsumoto, T., Akisue, T., Fujioka, H., Mizuno, K., Ohgushi, H., Wakitani, S., and Kurosaka, M. Treatment of a full-thickness articular cartilage defect in the femoral condyle of an athlete with autologous bone-marrow stromal cells. Osteoarthritis Cartilage **15,** 226, 2007.

4. Lee, K.B., Hui, J.H., Song, I.C., Ardany, L., and Lee, E.H. Injectable mesenchymal stem cell therapy for large cartilage defects—a porcine model. Stem Cells **25,** 2964, 2007.

5. Mauck, R.L., Yuan, X., and Tuan, R.S. Chondrogenic differentiation and functional maturation of bovine mesenchymal stem cells in long-term agarose culture. Osteoarthritis Cartilage **14,** 179, 2006.

6. Huang, A.H., Stein, A., Tuan, R.S., and Mauck, R.L. Transient exposure to transforming growth factor beta 3 improves the mechanical properties of mesenchymal stem cell-laden cartilage constructs in a density-dependent manner. Tissue Eng Part A **15,** 3461, 2009.

7. Shao, X.X., Goh, J.C.H., Hutmacher, D.W., and Lee, E.H. Repair of large articular osteochondral defects using hybrid scaffolds and bone marrow derived mesenchymal stem cells in a rabbit model. Tissue Eng **2,** 1539, 2006.

8. Ho, S.T., Hutmacher, D.W., Ekaputra, A.K., Hitendra, D., and Hui, J.H. The evaluation of a biphasic osteochondral implant coupled with an electrospun membrane in a large animal model. Tissue Eng Part A **16,** 1123, 2010.

9. Chan, B.P., and Leong, K.W. Scaffolding in tissue engineering: general approaches and tissue-specific considerations. Eur Spine J **Suppl 4,** 467, 2008.

10. Huang, A.H., Farrell, M.J., and Mauck, R.L. Mechanics and mechanobiology of mesenchymal stem cell-based engineered cartilage. J Biomech **43,** 128, 2010.

11. Raghunath, J., Rollo, J., Sales, K.M., Butler, P.E., and Seifalian, A.M. Biomaterials and scaffold design: key to tissue-engineering cartilage. Biotechnol Appl Biochem **46,** 73, 2007.

12. Moutos, F.T., Freed, L.E., and Guilak, F. A biomimetic three-dimensional woven composite scaffold for functional tissue engineering of cartilage. Nat Mater **6,** 162, 2007.

13. Xie, J., Ihara, M., Jung, Y., Kwon, I.K., Kim, S.H., Kim, Y.H., and Matsuda, T. Mechano-active scaffold design based on microporous poly(L-lactide-co-epsilon-caprolactone) for articular cartilage tissue engineering: dependence of porosity on compression force-applied mechanical behaviors. Tissue Eng **12,** 449, 2006.

14. Kang, Y., Yang, J., Khan, S., Anissian, L., and Ameer, G.A. A new biodegradable polyester elastomer for cartilage tissue engineering. J Biomed Mater Res A **77,** 331, 2006.

15. Li, C., Wang, L., Yang, Z., Kim, G., Chen, H., and Ge, Z. A viscoelastic chitosan-modified three-dimensional porous poly (L-lactide-co-ε-caprolactone) scaffold for cartilage tissue engineering. J of Biomater Sci Polym Ed **23,** 405, 2012.

16. Di Martino, A., Sittinger, M., and Risbud, M.V. Chitosan: a versatile biopolymer for orthopaedic tissue-engineering. Biomaterials **26,** 5983, 2005.

17. Neves, S.C., Moreira Teixeira, L.S., Moroni L., Reis, R.L., Van Blitterswijk, C.A., Alves, N.M., Karperien M., and Mano, J.F. Chitosan/poly(epsilon-caprolactone) blend scaffolds for cartilage repair. Biomaterials **32,** 1068, 2011.

18. Alves da Silva, M.L., Crawford, A., Mundy, J.M., Correlo, V.M., Sol, P., Bhattacharya, M., Hatton, P.V., Reis, R.L., and Neves, N.M. Chitosan/polyester-based scaffolds for cartilage tissue engineering: assessment of extracellular matrix formation. Acta Biomater **6,** 1149, 2010.

19. Yamamoto, A., Araki, T., Fujimori, K., Yamada, M., Yamaguchi, H., Izumi, K., *et al.* NaCl-aided Hoechst 33258 staining method for DNA quantification and its application. Histochemistry **92,** 65, 1989.

20. Hamid R., Rotshteyn Y., Rabadi L., Parikh R., and Bullock P. Comparison of alamar blue and MTT assays for high through-put screening. Toxicol In Vitro **18,** 703, 2004.

21. Mei, Y., Saha, K., Bogatyrev, S.R., Yang, J., Hook, A.L., Kalcioglu, Z.I., *et al.* Combinatorial development of biomaterials for clonal growth of human pluripotent stem cells. Nat Mater **9,** 768, 2010.

22. Ayala, R., Zhang, C., Yang, D., Hwang, Y., Aung, A., Shroff, S.S., *et al.* Engineering the cell-material interface for controlling stem cell adhesion, migration, and differentiation. Biomaterials **32,** 3700, 2011.

23. Woods, A., Wang, G., and Beier, F. Regulation of chondrocyte differentiation by the actin cytoskeleton and adhesive interactions. J Cell Physiol **213,** 1, 2007.

24. Kumar, D., and Lassar, A.B. The transcriptional activity of Sox9 in chondrocytes is regulated by RhoA signaling and actin polymerization. Mol Cell Biol. **29,** 4262, 2009.

25. Kim, D.K., Kim, S.J., Kang, S.S., and Jin, E.J. Curcumin inhibits cellular condensation and alters microfilament organization during chondrogenic differentiation of limb bud mesenchymal cells. Exp Mol Med **41,** 656, 2009.

26. Kim, D., Kim, J., Kang, S.S., and Jin, E.J. Transforming growth factor-beta3-induced Smad signaling regulates actin reorganization during chondrogenesis of chick leg bud mesenchymal cells. J Cell Biochem **107,** 622, 2009.

27. Tuli, R., Tuli, S., Nandi, S., Huang, X., Manner, P.A., Hozack, W.J., Danielson, K.G., Hall, D.J., and Tuan, R.S. Transforming growth factor-beta-mediated chondrogenesis of human mesenchymal progenitor cells involves N-cadherin and mitogen-activated protein kinase and Wnt signaling cross-talk. J Biol Chem **278,** 41227, 2003.

28. Hui, T.Y., Cheung, K.M., Cheung, W.L., Chan, D., and Chan, B.P. *In vitro* chondrogenic differentiation of human mesenchymal stem cells in collagen microspheres: influence of cell seeding density and collagen concentration. Biomaterials **29,** 3201, 2008.

29. Jung, Y., Kim, S.H., Kim, Y.H., and Kim, S.H. The effect of hybridization of hydrogels and poly(L-lactide-co-epsilon-

caprolactone) scaffolds on cartilage tissue engineering. J Biomater Sci Polym Ed **21,** 581, 2010.

30. Jung, Y., Park, M.S., Lee, J.W., Kim, Y.H., Kim, S.H., and Kim, S.H. Cartilage regeneration with highly-elastic three-dimensional scaffolds prepared from biodegradable poly(L-lactide-co-epsilon-caprolactone). Biomaterials **29,** 4630, 2008.

31. Xie, J., Han, Z., Naito, M., Maeyama, A., Kim, S.H., Kim, Y.H., and Matsuda, T. Articular cartilage tissue engineering based on a mechano-active scaffold made of poly(L-lactide-co-epsilon-caprolactone): *in vivo* performance in adult rabbits. J Biomed Mater Res B Appl Biomater **94,** 80, 2010.

32. Xie, J., Jung, Y., Kim, S.H., Kim, Y.H., and Matsuda, T. New technique of seeding chondrocytes into microporous poly(L-lactide-co-epsilon-caprolactone) sponge by cyclic compression force-induced suction. Tissue Eng **12,** 1811, 2006.

33. Ficklin, T., Thomas, G., Barthel, J.C., Asanbaeva, A., Thonar, E.J., Masuda, K., Chen, A.C., Sah, R.L., Davol, A., and Klisch, S.M. Articular cartilage mechanical and biochemical property relations before and after *in vitro* growth. J Biomech **40,** 3607, 2007.

34. Yan, D., Zhou, G., Zhou, X., Liu, W., Zhang, W.J., Luo, X., Zhang, L., Jiang, T., Cui, L., and Cao, Y. The impact of low levels of collagen IX and pyridinoline on the mechanical properties of *in vitro* engineered cartilage. Biomaterials **30,** 814, 2009.

35. Lee, H.J., Yu, C., Chansakul, T., Hwang, N.S., Varghese, S., Yu, S.M., and Elisseef, J.H. Enhanced chondrogenesis of mesenchymal stem cells in collagen mimetic peptide-mediated microenvironment. Tissue Eng Part A **14,** 1843, 2008.

36. Liu, S.Q., Tian, Q., Hedrick, J.L., Hui, J.H.P., Ee, P.L., and Yang, Y.Y. Biomimetic hydrogels for chondrogenic differentiation of human mesenchymal stem cells to neocartilage. Biomaterials **31,** 7298, 2010.

37. Wu, Y.N., Yang, Z., Hui, J.H.P., Ouyang, H.W., and Lee, E.H. Cartilaginous ECM component-modification of the micro-bead culture system for chondrogenic differentiation of mesenchymal stem cells. Biomaterials **28,** 4056, 2007.

38. Huang, A.H., Farrell, M.J., Kim, M., and Mauck, R.L. Long-term dynamic loading improves the mechanical properties of chondrogenic mesenchymal stem cell-laden hydrogel. Eur Cell Mater **19,** 72, 2010.

39. Jung, Y., Kim, S.H., Kim, S.H., Kim, Y.H., Xie, J., Matsuda, T., and Min, B.G. Cartilaginous tissue formation using a mechano-active scaffold and dynamic compressive stimulation. J Biomater Sci Polym Ed **19,** 61, 2008.

40. Jung, Y., Kim, S.H., Kim, Y.H., and Kim, S.H. The effects of dynamic and three-dimensional environments on chondrogenic differentiation of bone marrow stromal cells. Biomed Mater **4,** 055009, 2009.

Address correspondence to:
Zheng Yang, Ph.D.
NUS Tissue Engineering Program
National University of Singapore
27 Medical Drive
Singapore 117510
Singapore

E-mail: lsiyz@nus.edu.sg

Zigang Ge, M.D., Ph.D.
Department of Biomedical Engineering
College of Engineering
Peking University
Beijing 100871
P.R. China

E-mail: gez@pku.edu.cn